

MICROSTRUCTURE AND THERMAL CONDUCTIVITY OF $\text{AlN}(\text{Y}_2\text{O}_3)$ CERAMICSY. D. Yu,* A. M. Hundere,** R. Høier,* M. -A. Einarsrud[†], and R. E. Dunin-Borkowski^{††}

* Department of Physics, Norwegian University of Science and Technology, N-7491 Trondheim, Norway

**Elkem Refractories, Torshov, N-0402 Oslo, Norway

[†] Department of Chemistry, Norwegian University of Science and Technology, N-7491 Trondheim, Norway^{††} Department of Materials, Park Road, Oxford OX1 3PH, United Kingdom

Aluminum nitride (AlN) with high thermal conductivity has been considered as a potential substrate material for microelectronics. However, the thermal conductivity of polycrystalline AlN ceramics, prepared by liquid-phase sintering, is significantly lower than that of AlN single crystal. It has been shown that the thermal conductivity of AlN is inversely proportional to the oxygen content dissolved in the AlN lattice.¹ Furthermore, the microstructure of AlN can also influence the thermal conductivity considerably.² In the present study, we investigated the effect of grain boundaries and secondary phase distributions on thermal conductivity of two selected high density samples which contained similar oxygen content but showed different thermal conductivities.

Experimental details and selected properties of Samples A and B are shown in Table 1. Sample A with 0.8 wt% Y_2O_3 additive was embedded in an AlN powder bed in a BN crucible covered by a BN lid (not gas tight) during sintering, while Sample B with 3.9 wt% Y_2O_3 was embedded in an AlN powder bed in an open graphite crucible. Both samples were sintered in a graphite furnace under a nitrogen atmosphere at 1880°C for 2h.³ The thermal conductivity was measured using a laser flash method, and the oxygen content was measured using selective hot gas extraction method. Electron microscope observations were performed by using a JEOL JEM-3000F (equipped with a field-emission gun) and a Philips CM30, both of which were operated at an accelerating voltage of 300kV.

The microstructures of the samples were first investigated with a Philips CM30. Bright-field micrographs from both samples, which are shown in Figs. 1(a) and (b), reveal Y-containing secondary phases have dark contrast. Figure 1 also shows that some Y-containing secondary phases are formed along some of the AlN grain boundaries in Sample A, whereas they are primarily dispersed at isolated AlN grain junctions in Sample B. The structures of the secondary phases were determined from TEM diffraction pattern series through large-angle tilt. YAG ($\text{Al}_5\text{Y}_3\text{O}_{12}$) secondary phases were found to exist in both samples, while YAP (AlYO_3) secondary phase only was identified in Sample B. HRTEM studies of grain boundaries in the two samples were conducted using a JEOL JEM-3000F. Figures 2(a) and (b) show HRTEM images of vertical grain boundaries in Samples A and B, respectively. Comparing these two images in Figure 2, the grain boundaries in both samples seem clean without an obvious amorphous layer. However, EDS spectra obtained using a 0.6nm probe indicate that both boundaries have higher yttrium and oxygen contents than the adjacent grains, which implied a very thin amorphous layers still existed in the grain boundaries but could not be resolved in HRTEM images in Figure 2.

As shown in Table 1, both samples contain almost the same amounts of total oxygen and lattice dissolved oxygen, whereas the corresponding thermal conductivities are quite different. TEM observations suggest this phenomenon may be caused by the secondaries phase distribution along the grain boundaries or at isolated at grain junctions. The secondary phase with poor thermal conductivity distributed along the grain boundary would disrupt the connectivity of the high thermal conductivity AlN grains, such as shown in Fig.1(a), which were the main factors contributing to the decrease in the thermal conductivity of Sample A. As can be seen from Fig. 2(a), the low thermal conductivity Sample A also shows some grain boundaries that are almost without any secondary phase. However, it is proposed that grain with these kind boundaries do not form a continuous path for thermal conduction through the whole sample.

References

1. G. A. Slack et al., *J. Phys. Chem. Solids*, 48 (1987) 641.
2. H. Buhr and G. Müller, *J. Eur. Ceram. Soc.*, 12 (1993)271.
3. A.M. Hundere, and M.-A. Einarsrud, *J. Eur. Ceram. Soc.*, 16 (1996)899.
4. The authors thank the Norwegian Research Council for financial support, and Dr. J.L. Hutchison for permission to use JEOL JEM-3000F in Oxford.

Table 1. Experimental details and selected properties of AlN samples

Sample code	Wt % Y_2O_3	Sintering condition	Thermal Con. (W/mK)	Lattice oxygen content (wt %)	Total oxygen content (wt %)
A	0.8	BN crucible	91	0.56	1.32
B	3.9	C crucible	154	0.52	1.63

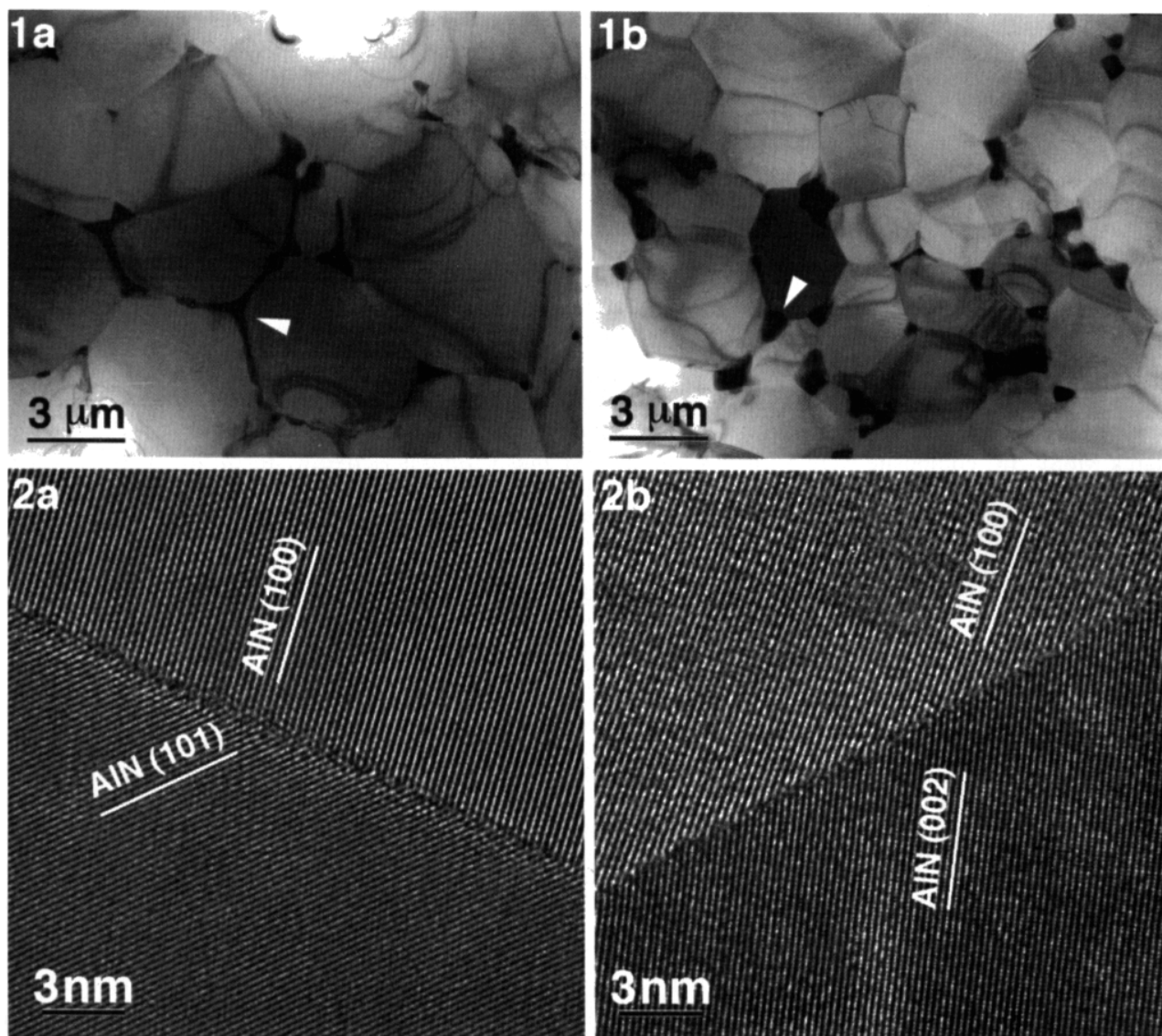


FIG. 1. Low magnification TEM bright-field images for (a) Sample A (the arrow shows dark secondary phase contrast formed along AlN boundaries), and (b) Sample B (the arrow shows secondary phase contrast at isolated AlN grain junctions).

FIG. 2. Representative HRTEM images of vertical AlN grain boundaries, with AlN grains close to low index planes. (a) Sample A; (b) Sample B.